DYNAMIC CORE STABILITY ANALYSIS OF A FLUIDIZED BED NUCLEAR REACTOR

V.V. Golovko, J.L. Kloosterman, H. van Dam, T.H.J.J. van der Hagen
Delft University of Technology
Interfaculty Reactor Institute (IRI)
Mekelweg 15
NL-2629 JB Delft, Netherlands
E-mail: v.golovko@iri.tudelft.nl, tel.: ++31 15 278 3623

ABSTRACT

A theoretical model describing the coupling of neutronics, thermohydraulics and the fluidization in a fluidized bed nuclear reactor is presented. The system of non-linear differential equations has been linearized near the operational working point of the reactor and Laplace transformed to obtain the transfer function from coolant mass-flow rate to reactor power. All the poles of the transfer function have negative real parts for the whole operational regime of the coolant flow rate, which indicates a stable behavior of the reactor within the limits of the linearized model.

1. INTRODUCTION

FLUBER is a conceptual design of a fluidized bed nuclear reactor that consists of TRISO coated fuel particles contained in a graphite-walled cavity. The outer diameter of each fuel particle is 1 mm, the horizontal cross section of the core cavity is 1 m^2 and its height is 6 m. The thickness of both the axial and the radial graphite reflectors is 1 m. Helium is used as a coolant. When the coolant starts to flow upwardly, the particle bed gets fluidized and reactivity increases due to the influence of the reflector. The maximum reactivity that can be introduced in this way is limited, because the reactor becomes subcritical again due to increased neutron leakage when the particle bed expands further. As a result, the reactor is critical only for a specific range of coolant flow rates, which inherently limits the maximum power that can be generated. A more detailed description of the reactor is given in Refs. 1 and 2.

The reactivity of the reactor strongly depends on the core expansion that depends on the mass flow rate and the temperature of the coolant. Therefore, the interaction between the fluidization process, the thermohydraulics and the nuclear kinetics is very important for the stability of the reactor.

In recent years much research has been performed in the field of dynamic stability of nuclear reactors, especially on the coupling between neutronics and the thermohydraulics processes of conventional reactors. The mathematical model describing the process in FLUBER consists of coupled neutronics and thermohydraulics models that are also used for the stability analysis in conventional reactors, and a fluidization model to describe the fluidization processes in the active core.

After describing the combined mathematical models in section 2, we introduce the "linearized" coupled model in section 3, parameters of the models in section 4. The linear stability analysis is also shown in section 4. Main results and discussions are given in the final section.

2. COUPLED NEUTRONIC-THERMOHYDRAULICS AND FLUIDIZATION MODEL

2.1 FLUIDIZATION BED MODEL

Fluidization is a suspension of fuel particles in an upwardly flowing fluid, producing a fluidized bed. Fluidization can be classified by the number of phases involved. The present paper is concerned with two-phase fluidization: a solid and a gas (helium).

On the vertically upwards flow of a coolant, a columnar fixed bed undergoes little visible change with increasing superficial velocity of the continuous phase, U, until it reaches the minimum fluidization velocity for a two-phase bed, U_m, at which the bed becomes fluidized. In reality the fluidization process is not clear-cut, but occurs over a range of velocities due to particle clusters and channeling. Ergun[3] gives the pressure drop per unit length of the fluidized bed, Dp/H, as the sum of that due to viscous and kinetic energy losses:

$$\frac{\Delta p}{H} = \frac{150h}{d_f^2}\frac{(1-e)^2}{e^3}U + \frac{1.75r_c}{d_f}\frac{(1-e)}{e^3}U^2, \tag{1}$$

where h is the fluid dynamic viscosity, d_f is the fuel particle diameter, r_c is the coolant density, and e is the bed void fraction. At minimum fluidization, the pressure drop exactly balances the buoyant weight of the material:

$$\frac{\Delta p}{H} = (1-e)(r_f - r_c)g, \tag{2}$$

where r_f (2725 kg·m^{-3}) is the coated-fuel particle density and g is the acceleration due to gravity. Equating (1) and (2) gives the minimum fluidization velocity U_m. In a column with flow velocities greater than the minimum, a further increase of the coolant velocity will cause the bed to expand (void fraction increases) with a constant pressure drop. Generally, columnar expansion follows the relation of Richardson and Zaki[3]:

$$U = U_t e^n \tag{3}$$

where U_t is the effective terminal velocity of the gas at maximal porosity and n is the Richardson-Zaki constant. For the experimentally determined values of the minimum fluidization point for gas-particle fluidization, the value of n in Eq. (3) decreases from 3.14 to 1.58 (see Ref. 4). So, the exponent n in the Richardson-Zaki correlation is not a constant value, but at the best, the exponent is constant over a limited range of the gas velocity. For our analysis we used a constant

value of 2.4 for the whole operational regime of FLUBER. For the turbulent regime, assuming that all fuel particles have an ideal spherical form, the terminal velocity can be calculated by:

$$U_t = \sqrt{\frac{4gd_f\left(r_f - r_c\right)}{3c_D r_c}} \tag{4}$$

where c_D is the drag coefficient that depends on the characteristics of the particles. Although the experiment shows that the drag coefficient for spherical particles varies as a function of the gas velocity, it was taken constant and equal to 0.445 for the entire operational turbulent regime of the reactor.

The above relation between U and e (Eq. 3) was chosen because of its good agreement with published experimental data[4]. Experimental data have demonstrated that the void fraction-gas velocity relationship for a gas-particle fluidization is independent of the total mass of the particles and of the fluidizing tube diameter if the tube-to-particle diameter is larger than 20 (see Ref. 5). Here this ratio is larger than 1000. The void fraction at the minimum fluidization velocity is equal to 0.48, which corresponds to a cubic-packed columnar bed.

The movement of the particles in the core is highly turbulent. The void fraction remains in the range of 0.48 to 0.87 that corresponds to expanded core heights of 136 cm and 544 cm, respectively. The bed is assumed to expand uniformly and continuously as the coolant velocity increases.

2.2 THERMAL HYDRAULICS MODEL

For our analysis we consider two regions in FLUBER (fuel particles and coolant), each characterized by a space-average temperature. Writing energy balances for the active core zone, we get the equations for the so-called “lumped-parameter” temperatures:

$$\begin{aligned}(mc)_f \frac{dT_f}{dt} &= P - hA_f\left(T_f - T_c\right)\\ (mc)_c \frac{dT_c}{dt} &= hA_f\left(T_f - T_c\right) - Gc_c\left(T_{out} - T_{in}\right)\end{aligned} \tag{5}$$

where T_f and T_c are the temperatures of the fuel particles and the coolant, P is the power of the reactor, h is the heat transfer coefficient from particles to fluid, A_f is the heat transfer area of all the fuel particles in the core (4272.36 m^2), G is the mass flow rate of the helium through the core, $(mc)_f$ and $(mc)_c$ are the total heat capacities of all the particles and all the helium in the active core region, respectively, c_c is the specific heat capacity of the coolant (5193 $J{\cdot}kg^{-1}K^{-1}$), T_{out} is the outlet temperature of the coolant, and T_{in} is the inlet temperature of the gas chosen as 543 K. Although the heat transfer coefficient strongly depends on the flow rate and the thermal properties of the coolant, here we use a constant value of $7.7{\cdot}10^3$ $W{\cdot}m^{-2}K^{-1}$ (see Ref. 6). Assuming that the coolant temperature has a point-symmetric distribution relative to the active core mid-plane, we can rewrite the second expression in Eq. (5) as:

$$(mc)_c \frac{dT_c}{dt} = hA_f\left(T_f - T_c\right) - Gc_c 2\left(T_c - T_{in}\right). \tag{6}$$

Because the coolant behaves like a thermally perfect gas, the equation of state writes:

$$r_c = \frac{pM}{RT_c} \tag{7}$$

where p is the pressure of the helium, M is the molar mass of the helium and R is the gas constant. As was mentioned above, the pressure drop during fluidization remains constant, which implies that, the "lumped" gas pressure does not change in the whole range of operational expansion of the fluidized bed.

2.3 NEUTRON KINETICS MODEL

The ordinary point-kinetic equations with one delayed-neutron group describe the time-dependent behavior of the reactor power and precursor concentration:

$$\begin{aligned} \frac{dP}{dt} &= \frac{r-b}{\Lambda} P + l C \\ \frac{dC}{dt} &= \frac{b}{\Lambda} P - l C \end{aligned} \tag{8}$$

where C is the precursor density (expressed in latent power; same units as P), r is the reactivity, b is the delayed-neutron fraction (0.69 %), L is the mean neutron-generation time ($2.0 \cdot 10^{-3}$ s), and l is the precursor decay constant for one-group of delayed neutron (0.079 s^{-1}). The fluidized bed model is coupled to the point-kinetics model and the thermal-hydraulics model by

$$r = r(e) + a_D \left(T_f - T_{f0} \right) \tag{9}$$

where a_D is the reactivity coefficient of fuel temperature that is assumed not to depend on the void fraction, T_{f0} is the reference temperature of the fuel particles, $r(e)$ is the reactivity as a function of void fraction (or expanded core height)[2] adequately approximated with a four-term polynomial:

$$r(e) = \sum_{i=0}^{i=4} a_i e^i \tag{10}$$

where a_i are the fit coefficients.

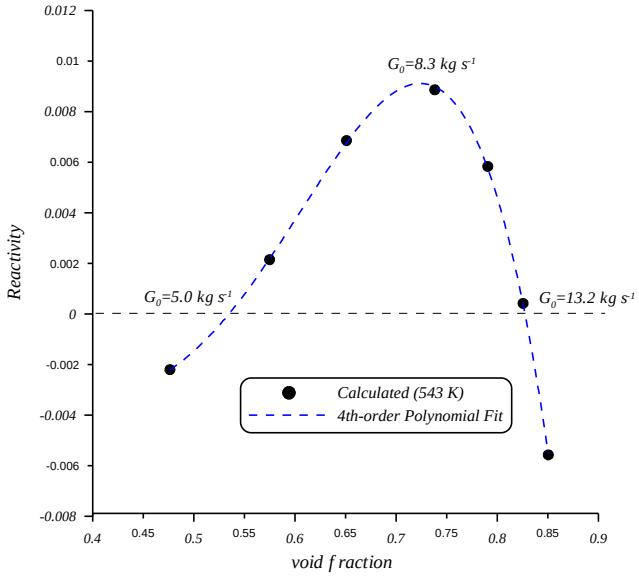

Figure 1. The reactivity as a function of the void fraction in the active core[2] calculated by the two-dimensional diffusion code BOLD-VENTURE.

Figure 1 shows that the reactivity increases up to a maximum at a void fraction of 0.74, which corresponds to a core height of 270 cm. When the expansion of the core continues and the void fraction further increases, reactivity decreases again. For a void fraction between 0.48 to 0.74, neutrons that leak away from the core are effectively moderated in the surrounding graphite and reflected into the core, which gives a gain in reactivity. However, for void fractions larger than 0.74, too many neutrons that leak away are absorbed in the graphite reflector.

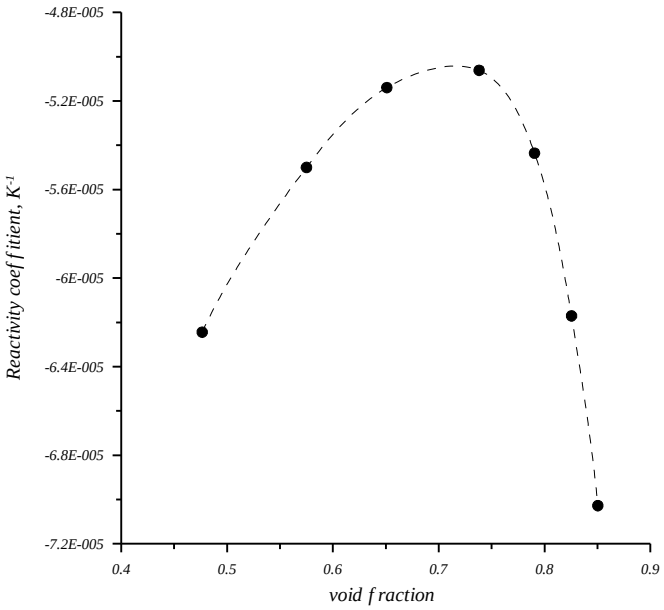

Figure 2. The reactivity coefficient of fuel temperature as a function of the void fraction of the active core zone. Calculations of the effective multiplication factor of the FLUBER were done by diffusion code BOLD VENTURE for the reference temperature 543 K and for the 843 K. The dashed line is just to guide the eye.

Figure 2 shows that the fuel temperature coefficient varies with the void fraction. In the analysis described in section 4, we used a conservative value of $-5 \cdot 10^{-5}$ K^{-1} that is assumed not to depend on the void fraction of the active core zone.

3. LINEARIZED COUPLED MODEL OF FLUBER

To investigate linear stability, we must reduce Eqs. (3) through (9) to a set of linear equations correct to first-order in the deviations from equilibrium. Using the superscript zero to denote the values at the stationary state, we rewrite our combined model in a linear form expanding the nonlinear terms in powers and retaining only the linear terms. Using Laplace transformation we obtain the transfer function from mass flow rate to reactor power.

3.1 LINEARIZED FLUIDIZATION MODEL

For simplicity, we assume that the helium density is negligible compared to the fuel particle density ($r_f >> r_c$). In this case the formula for terminal velocity (Eq. 4) can be rewritten as:

$$U_{t0} = \sqrt{\frac{4gd_f r_f}{3c_D r_{c0}}}\,. \tag{11}$$

Close to the stationary working point we can expand the nonlinear terms in powers. This gives us the next set of linear expressions (the local pressure is assumed to be constant in the whole operational range of FLUBER).

$$dG = G_0\left(\frac{dr_c}{r_{c0}} + \frac{dU}{U_0}\right) \qquad dr_c = -r_{c0}\frac{dT_c}{T_{c0}} \tag{12}$$

$$de = \frac{e_0}{n}\left(\frac{dU}{U_0} - \frac{dU_t}{U_{t0}}\right) \qquad dU_t = -\frac{1}{2}U_{t0}\frac{dr_c}{r_{c0}} \tag{13}$$

where the subscript zero denotes the equilibrium state in this case:

$$G_0 = r_{c0}U_0 A \qquad r_{c0} = \frac{pM}{RT_{c0}} \qquad e_0 = \left(\frac{U_0}{U_{t0}}\right)^{\frac{1}{n}} \tag{14}$$

where A is the cross-sectional area of the active core (1 m^2). The coolant temperature T_{c0} represents the equilibrium temperature obtained by setting $dT_c/dt=0$ and $dT_f/dt=0$ in Eq. (5) at a steady power level P_0. So, we get

$$T_{c0} = T_{in} + \frac{P_0}{2G_0 c_c} \qquad T_{f0} = T_{in} + P_0\left(\frac{1}{2G_0 c_c} + \frac{1}{hA_f}\right) \tag{15}$$

3.2 LINEARIZED THERMAL-HYDRAULICS MODEL OF FLUBER

Let us consider small fluctuations of the reactor power, the space-average fuel temperature, the space-average coolant temperature, and the mass-flow rate near the equilibrium point. We assume $T_f=T_{f0}+dT_f$, $T_c=T_{c0}+dT_c$, $G=G_0+dG$, and $P=P_0+dP$. Substituting in Eq. (5) and neglecting second-order terms one gets:

$$\begin{aligned}(mc)_f\frac{d}{dt}dT_f &= dP - hA_f\left(dT_f - dT_c\right),\\ (mc)_c\frac{d}{dt}dT_c &= hA_f\left(dT_f - dT_c\right) - 2dGc_c\left(T_{c0} - T_{in}\right) - 2G_0c_c dT_c.\end{aligned} \tag{16}$$

Using the integral Laplace transformation we can rewrite (16) in the form:

$$\begin{aligned}d\tilde{T}_f &= d\tilde{P}\frac{b_1}{s+h_1} + d\tilde{T}_c\frac{h_1}{s+h_1}\\ d\tilde{T}_c &= d\tilde{G}\frac{b_2}{s+h_2+h_3} + d\tilde{T}_f\frac{h_2}{s+h_2+h_3}\end{aligned} \tag{17}$$

where '~' denotes the a Laplace transformed variable and the $b_{1,2}$ and $h_{1..3}$ symbols are positive constants:

$$b_1 = \frac{1}{(mc)_f} \qquad b_2 = \frac{2c_c\left(T_{c0} - T_{in}\right)}{(mc)_c}$$
$$h_1 = \frac{hA_f}{(mc)_f} \qquad h_2 = \frac{hA_f}{(mc)_c} \qquad (18)$$
$$h_3 = \frac{2G_0 c_c}{(mc)_c}$$

3.3 LINEARIZED NEUTRON KINETICS MODEL

The linerization of the neutron-kinetics model is described in more detail in Ref. 7. In this section we present the zero-power reactor transfer function H_1. For this study we assume the reactor to be critical, which simplifies the zero-power reactor transfer to:

$$H_1 = \frac{P_0\left(s+l\right)}{\Lambda s\left(s+l+b/\Lambda\right)} \approx \frac{P_0\left(s+l\right)}{\Lambda s\left(s+b/\Lambda\right)}, \qquad (19)$$

where we neglected the term l in the denominator because $l << b/L$.

As we already noted above, the neutronics, thermal-hydraulics, and fluidization models are coupled by the reactivity that, after linerization, can be expressed by:

$$dr = \left(\sum_{i=1}^{i=4} i a_i e_0^{i-1}\right) de + a_D dT_f . \qquad (20)$$

3.4 BLOCK DIAGRAM

We illustrate the physical processes involved in the dynamics of FLUBER by following the consequences of a hypothetical coolant flow rate increase. An elementary block diagram describing the dynamics of FLUBER is presented in Fig. 3. Here, each block represents a transfer functions between two variables of the coupled model.

When the helium mass flow rate increases, the void fraction in the core increases, which will change the power of the reactor. The variation of the power leads to a shift of the mean fuel temperature that, through Doppler reactivity feedback, affects the reactor power. Furthermore, the changing particle temperature leads to a change of the helium temperature, and through a change of the coolant density, of the reactivity. Altogether, it provides a combined model for an elementary dynamic analysis of the physical processes in FLUBER.

From the linearized equations we find the transfer functions between the variables shown in Fig. 3 and the `overall` transfer function from coolant flow rate to reactor power:

$$Y(s) = \frac{d\tilde{P}}{d\tilde{G}} = \frac{H_1\left(H_2\left(H_4\left(H_8\left[1-H_{12}H_{13}\right]+H_7H_{11}H_{10}\right)+H_5H_9H_{10}H_{11}\right)+H_3H_{11}H_{12}\right)}{1-H_{12}H_{13}-H_1H_6\left(H_2H_{13}\left[H_4H_7H_{10}+H_5H_9H_{10}\right]+H_3\right)} \qquad (21)$$

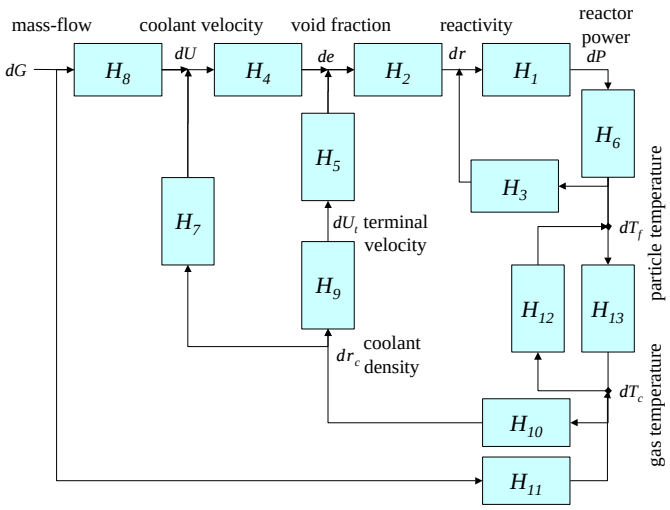

Figure 3. The elementary block diagram of the mathematical model of the reactor. Each block denotes a relation between two variables.

Now we have to find all the poles of the transfer function. Substituting the nomenclatures of the transfer functions shown in Table I into Eq. (21), then expanding the nominator and the denominator of the transfer function, and equating the nominator to zero, we find:

$$\left(1-\frac{h_1h_2}{(s+h_1)(s+h_2+h_3)}-\frac{P_0(s+l)}{s(s\Lambda+b)}\frac{b_1}{(s+h_1)}\left[\frac{3h_1\left(\sum_{i=1}^{i=4}ie_0^ia_i\right)e_0}{2(s+h_1)nT_{c0}}+a_D\right]\right)(s+h_2+h_3)=0. \quad (22)$$

Table I. Nomenclature of various transfer functions.

Transfer Functions			
$H_1=\frac{P_0(s+l)}{\Lambda s(s+b/\Lambda)}$	Zero-power reactivity to power	$H_2=\sum_{i=1}^{i=4}ie_0^{i-1}a_i$	Void fraction to reactivity
$H_3=a_D$	Fuel temperature to reactivity	$H_4=\frac{e_0}{nU_0}$	Coolant velocity to void fraction
$H_5=-\frac{e_0}{nU_{t0}}$	Gas terminal velocity to void fraction	$H_6=\frac{b_1}{s+h_1}$	Reactor power to fuel particle
$H_7=-\frac{U_0}{r_{c0}}$	Coolant density to gas velocity	$H_8=\frac{U_0}{G_0}$	Gas velocity to coolant mass-flow
$H_9=-\frac{U_{t0}}{2r_{c0}}$	Coolant density to gas terminal velocity	$H_{10}=-\frac{r_{c0}}{T_{c0}}$	Gas temperature to coolant density
$H_{11}=\frac{b_2}{s+h_2+h_3}$	Coolant mass-flow to gas temperature	$H_{12}=\frac{h_2}{s+h_2+h_3}$	Coolant temperature to fuel temperature
$H_{13}=\frac{h_1}{s+h_1}$	Fuel temperature to coolant temperature		

4. LINEAR SYSTEM STABILITY

The poles of the transfer function characterize the dynamics response of a linear system. If at least one pole has a positive real part, the response to a perturbation will grow indefinitely and the linear system is unstable. If all the poles have negative real parts, the response to a perturbation will decay to zero as $t \to \infty$. The system returns close to its equilibrium and is asymptotically stable. In the root-locus method, the poles of the transfer function are investigated by determining how these poles change position in the s-plane when only one parameter is varied. A stable linear system becomes unstable when a pole (or a pair of complex conjugate poles) crosses the imaginary axis in the s-plane. As the parameter for the root-locus analysis we chose the coolant mass flow rate G_0.

Figure 4 shows the equilibrium reactor power and the equilibrium fuel temperature as a function of the coolant mass flow rate. These results were numerically calculated in the time domain in response to a step transient in the coolant mass flow rate. After all transient processes died out ($t \to \infty$), the reactor power and the mean fuel temperature reached their equilibrium values that are plotted in Fig. 4 versus the equilibrium coolant mass-flow rate. The behavior of the steady state reactor power as a function of coolant flow is very similar to Fig. 1 that shows the reactivity of the reactor as a function of the void fraction. At a coolant mass flow rate of about 9 $kg \cdot s^{-1}$, the equilibrium reactor power has a maximum, which corresponds approximately with the maximum reactivity that can be introduced (see Fig. 1). For a lower mass flow rate, the reactor power increases with the mass flow rate, while for values of the mass flow rate larger than 9 $kg \cdot s^{-1}$ the opposite is true. The results of the steady state reactor power are adequately approximated with a four-order polynomial to be used for constructing the root-locus.

Figure 5 shows the root-locus plot of all the poles of the transfer function from coolant mass flow rate to reactor power for the whole operational regime of the coolant mass flow rate in FLUBER. The poles differ many orders in magnitude, because the parameters used in the model are so widely spread. Figure 5 shows that each pole of the transfer function has a negative value, however, it is difficult to see how each pole varies with the coolant mass flow rate. As mentioned before, the real part of each pole of the transfer function determines the decaying or increasing response of the reactor upon an external reactivity perturbation. Therefore, it is interesting to see separately how the real and imaginary parts of the poles change as a function of the coolant mass flow rate.

Figure 6 illustrates the behavior of the real part of each pole and of the imaginary part of poles 4 and 5 as a function of the coolant flow rate. Poles 4 and 5 become complex conjugates of each other for values of the flow rate between 9.7 and 11.2 $kg \cdot s^{-1}$. When two poles are complex conjugates of each other, the impulse response of the linearized system shows an exponentially decreasing or increasing sinusoidal behavior. The ratio between two consecutive maximal values of this function is called the decay ratio given by:

$$DR = \exp\left(\frac{2\pi\sigma}{|\omega|}\right) \tag{23}$$

where σ and ω are the real and the imaginary parts of the conjugate poles. However, in our case the ratio of the real and the imaginary parts is so strongly negative (see Fig. 6) that the DR has a negligible small value so that effectively no oscillatory behavior can be observed.

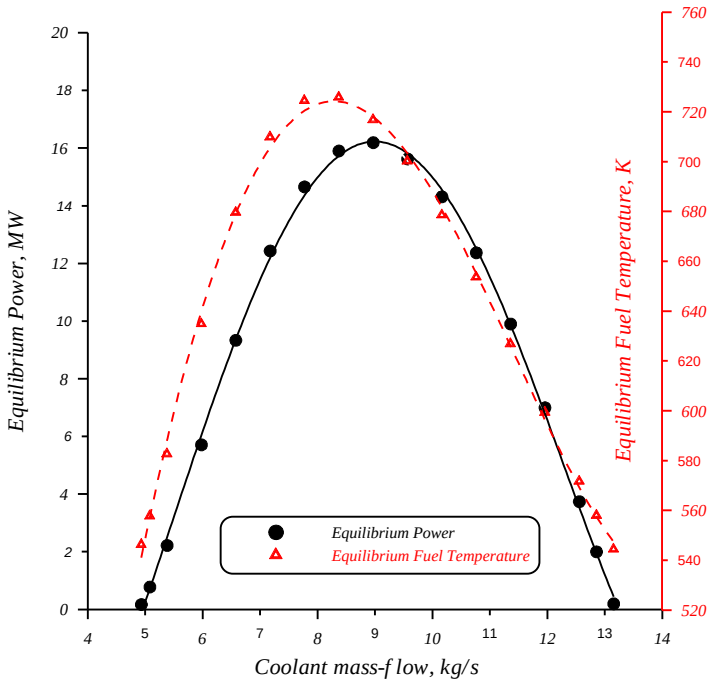

Figure 4. The stationary values of the reactor power and the fuel particle temperature as a function of the coolant mass-flow rate. The solid black line shows the 4th-order polynomial fit of the equilibrium reactor power as a function of the coolant mass flow rate that we use in our analysis. The actual value of the equilibrium reactor power depends of course on the inventory and the composition of the fuel in the core.

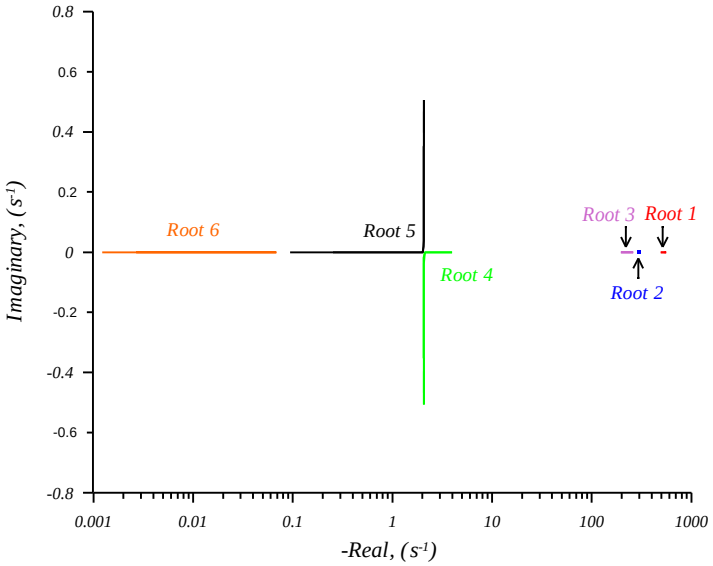

Figure 5. The Root-locus plot of all the poles of the transfer function from coolant mass flow to reactor power for the whole operational regime of FLUBER. The green and black lines represent pairs of complex conjugates. The three other poles are real.

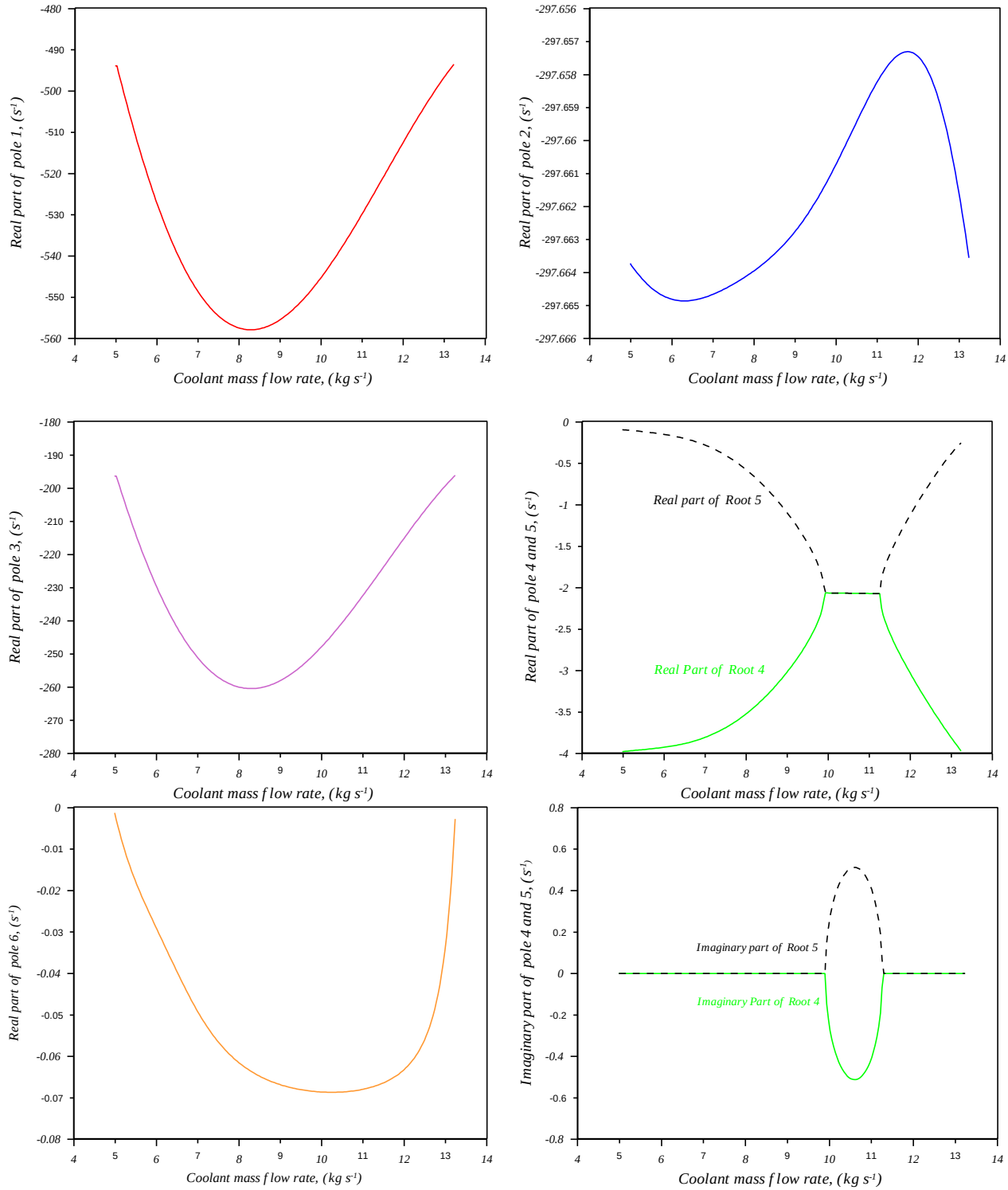

Figure 6. The real part of each pole and the imaginary part of poles 4 and 5 of the transfer function from coolant mass flow rate to reactor power for the whole operational regime of FLUBER. All poles have a negative real part that indicates a stable behavior of the reactor within the limit of the linearized coupled model.

5. CONCLUSIONS

A theoretical model is presented describing the neutronics, thermohydraulics and the fluidization processes in a fluidized bed nuclear reactor. The neutronics model consists of a point-kinetics model with one effective delayed neutron group. The thermohydraulics model is also a lumped parameter model that describes the fuel and coolant temperatures as a function of reactor power and the coolant mass flow rate. Furthermore, it gives the density of the coolant as a function of its temperature. The fluidization model, finally, describes the gas coolant velocity as a function of the void fraction in the core and the density of the coolant.

The three models have been coupled and linearized around the steady-state working points of the reactor. The linearized model has been Laplace transformed to obtain the transfer function from the coolant mass flow rate to reactor power. Root-locus analysis of this transfer function with the inlet coolant mass flow rate as the parameter that has been varied, shows that all poles have strong negative real parts, which indicates that the reactor is very stable (strongly damped) in the range of all operational values of the coolant mass flow rate. Furthermore, no oscillatory behavior can be observed.

The maximum power that can be generated with the reactor model studied is about 16 MW_{th} at a coolant mass flow rate of about 9 $kg \cdot s^{-1}$, but enlarging or reducing the fuel inventory of the system can be used to modify the maximum power. The influence of the core inventory on the stability of the reactor has yet to be studied, as well as the influence of varying other parameters in the root-locus analysis like coolant inlet temperature. The thermal efficiency of the reactor is expected to be very high due to the excellent heat transfer from the fuel particles to the coolant. Effectively, the coolant temperature equals that of the fuel.

REFERENCES

1. H. van Dam, T.H.J.J. van der Hagen, J.E. Hoogenboom, V.A. Khotylev, R.F. Mudde, *Statics and Dynamics of a Fluidized Bed Fission Reactor*, Proc. ICENES'98, Tel Aviv, June 28-July 2, pp 609-616 (1998).
2. J.L. Kloosterman, H. van Dam, V.V. Golovko, T.H.J.J. van der Hagen, *Neutronic Design of a Fluidized Bed Reactor*, GLOBAL'99, August 29-September3, 1999.
3. W.J. Beek, K.M.K. Muttzall, *Transport Phenomena*, John Wiley & Sons LTD, New York, 1975.
4. P.E.A. Rots, *Feasibility Study of a Fluidized Bed Nuclear Fission Reactor*, final report, Delft University of Technology and Kramers Laboratorium voor Fysische Technologie, Delft, The Netherlands, September 20, 1995.
5. J.F. Davidson, R. Clift, D. Harrison, *Fluidization. Second Edition*, Academic Press, New York 1985.
6. G. Melese and R. Katz, *Thermal and Flow Design of Helium-Cooled Reactors*, ANS, LaGrange Park, 1984.
7. D.L. Hetrick, *Dynamics of Nuclear Reactors*, ANS, Illinois USA, 1993.